Article:
Margulies, Daniel S, Ghosh, Satrajit S, Goulas, Alexandros et al. (9 more authors) (2016) Situating the default-mode network along a principal gradient of macroscale cortical organization. Proceedings of the National Academy of Sciences of the United States of America. pp. 12574-12579. ISSN 1091-6490

https://doi.org/10.1073/pnas.1608282113

Situating the default-mode network in a principal gradient of macroscale cortical organization

Daniel S. Margulies[a,1], Satrajit S. Ghosh[b,c], Alexandros Goulas[d], Marcel Falkiewicz[a], Julia M. Huntenburg[a,e], Georg Langs[f], Gleb Bezgin[g], Simon Eickhoff[h,i], F. Xavier Castellanos[j], Michael Petrides[k], Elizabeth Jefferies[l], and Jonathan Smallwood[l]

[a]Max Planck Research Group for Neuroanatomy & Connectivity, Max Planck Institute for Human Cognitive and Brain Sciences, Leipzig, 04103, Germany; [b]McGovern Institute for Brain Research, MIT, Cambridge, MA, 02139, USA; [c]Department of Otolaryngology, Harvard Medical School, MA, 02115, USA; [d]Department of Computational Neuroscience, University Medical Center Hamburg-Eppendorf, Hamburg, 20246, Germany; [e]Neurocomputation and Neuroimaging Unit, Department of Education and Psychology, Free University of Berlin, 14195, Berlin, Germany; [f]Department of Biomedical Imaging and Image-guided Therapy, CIR Lab, Medical University of Vienna, Vienna, A-1090, Austria; [g]Cognitive Neuroscience Unit, Montreal Neurological Institute, McGill University, Montreal, H3A 2B4, Canada; [h]Institute for Neuroscience and Medicine (INM-1), Research Center Jülich, Jülich, 52428, Germany; [i]Institute of Clinical Neuroscience and Medical Psychology, Heinrich-Heine University, Düsseldorf, 40225, Germany; [j]Child Study Center, Department of Child and Adolescent Psychiatry, NYU Langone Medical Center, NY, 10016, USA; [k]McConnell Brain Imaging Centre, Montreal Neurological Institute, McGill University, Montreal, H3A 2B4, Canada; [l]Department of Psychology and York Neuroimaging Centre, University of York, York, YO10 5DD, United Kingdom

This manuscript was compiled on August 24, 2016

Understanding how the structure of cognition arises from the topographical organization of the cortex is a primary goal in neuroscience. Previous work has described local functional gradients extending from perceptual and motor regions to cortical areas representing more abstract functions, yet an overarching framework for the association between structure and function is still lacking. Here we show that the principal gradient revealed by the decomposition of connectivity data in humans and the macaque monkey is anchored, at one end, by regions serving primary sensory/motor functions and, at the other, by transmodal regions that, in humans, are known as the default-mode network (DMN). These DMN regions exhibit the greatest geodesic distant along the cortical surface — and are precisely equidistant — from primary sensory/motor morphological landmarks. The principal gradient also provides an organizing spatial framework for multiple large-scale networks and characterizes a spectrum from unimodal to heteromodal activity in a functional meta-analysis. Together these observations provide a novel characterization of the topographical organization of cortex and indicate that the role of the DMN in cognition might arise from its position at one extreme of a hierarchy, allowing it to process transmodal information that is unrelated to immediate sensory input.

topography | connectivity | cortical organization | default-mode network

A key assumption in neuroscience is that the topographical structure of the cerebral cortex provides an organizing principle that constrains its cognitive processes. Recent advances in the field of human connectomics have revealed multiple large-scale networks [e.g., 1–3], each characterized by distinct functional profiles [4]. Some are related to basic primary functions, such as moving or perceiving sounds and images; some serve well-documented, domain-general functions, such as attention or cognitive control [5–8]; and some have functional characteristics that remain less well understood, such as the default-mode network (DMN) [9, 10]. Although the topography of these distinct distributed networks has been described using multiple methods [e.g., 1–3], the reason for their particular spatial relationship and how this constrains their function remains unclear.

Advances in mapping local processing streams have revealed spatial gradients that support increasingly abstract levels of representation, often extending along adjacent cortical regions in a stepwise manner [11]. In the visual domain, for example, the ventral occipito-temporal object stream transforms simple visual features, coded by neurons in primary visual cortex, into more complex visual descriptions of objects in anterior inferior temporal cortical regions, and ultimately contributes to multimodal semantic representations in the middle temporal cortex and the most anterior temporal cortex that capture the meaning of what we see, hear and do [12–15]. Similarly, in the prefrontal cortex, a rostral-caudal gradient has been proposed whereby goals become increasingly abstract in anterior areas more distant from motor cortex, as they are increasingly removed from selection processes that operate on specific motor representations [5, 16–19]. Much like the function–structure correspondence elucidated by topographic maps within sensory and motor areas [20, 21], these processing gradients provide a systematic mapping between spatial position and a functional spectrum of increasingly abstract representation [22].

Processing gradients have proven useful for understanding the relation between specific regions and function in separate domains; Mesulam observed that the emergence of more abstract functional classes of cortex may follow a similar trajectory, hypothesizing that abstract categories emerge from the convergence of information across modalities [23, and see Figure 1C]. This notion has recently been extended by Buckner and Krienen [24], who proposed the 'tethering hypothesis', arguing that association cortex gains its functional attributes

Significance Statement

We describe an overarching organization of large-scale connectivity that situates the default-mode network at the opposite end of a spectrum from primary sensory and motor regions. This topography, based on the differentiation of connectivity patterns, is also embedded in the spatial distance along the cortical surface between these respective systems. In addition, this connectivity gradient accounts for the respective positions of canonical networks and captures a functional spectrum from perception and action to more abstract cognitive functions. These results suggest that the default-mode network consists of regions at the top of a representational hierarchy that describe the current cognitive landscape in the most abstract terms.

DSM, MP, EJ, JS, Conception and design, Analysis and interpretation of data, Drafting or revising the article; SSG, AG, MF, JMH, GL, SE, FXC, Analysis and interpretation of data, Drafting or revising the article; GB, Contributed unpublished, essential data, or reagents.

The authors declare that no competing interests exist.

[1]To whom correspondence should be addressed. E-mail: margulies@cbs.mpg.de

through its increasing spatial distance from the constraints that determine the functional specialization of primary cortex. These viewpoints suggest that there may be macroscale gradients that integrate information across multiple domains into progressively more abstract representations, in which local gradients within specific cortical systems could be situated and understood.

One large-scale cortical system whose function remains unclear is the DMN. Initially identified through its tendency to deactivate during externally-oriented tasks [25], the DMN has since been shown to activate in tasks that depend on information retrieved from memory such as remembering the past or thinking about the future, or considering the mental states of others (for reviews, see [10, 26]). The DMN is also known to play a role in states that are less related to ongoing environmental events, such as daydreaming and mind-wandering [27–30], and contributes to lapses in the integrity of external processing [31]. A consensus view on the role of the DMN in human cognition is still lacking, however, because of the increasing number of cognitive domains in which it has been implicated. As well as playing an active role during states such as autobiographical memory retrieval, social cognition, and future thinking, the DMN has recently been shown to operate in concert with regions implicated in cognitive control during complex working memory tasks [32–36]. This emerging evidence illustrates that the DMN is not tied to a specific form of informational content, leading to suggestions that it acts as a hub that integrates representational information across the cortex [30, 37].

To understand the topographic organization of the cerebral cortex at the macroscale [38], we explore how the principal variance in cortical connectivity relates to the topography of structure and function by addressing four key questions: (a) Is there a macroscale gradient of connectivity in the human brain that reflects the systematic integration across modalities in a hierarchical fashion? (b) Does this macroscale organization relate to the geometric structure of the cortex? (c) Does the organization captured by the principal gradient account for the spatial distribution of large-scale networks and the associated functions across the cortex? (d) Do these observations provide a framework for understanding the functional role of the DMN in cognition?

Results

We began our analysis by characterizing the components describing the maximum variance in functional connectivity patterns — the extent to which nodes agree in the spatial distribution of correlations — across the human cerebral cortex (Figures 1 & S2). The functional connectivity matrix consisted of 91282 cortical and subcortical 'grayordinates' with a resolution of 2 mm from the preprocessed dense connectome S900 release of the Human Connectome Project (HCP) [39]. These data were based on one hour of resting-state fMRI data acquired from 820 healthy adult individuals. No further processing of the connectivity matrices beyond those already implemented by the HCP, which included minimal spatial smoothing of 2 mm FWHM [40], were conducted.

Rather than delineating discrete network parcellations, we implemented a method that captures gradients in connectivity patterns over space — a cortical feature, termed 'connectopies' [41]. This method, known as diffusion embedding [42], allows local and long distance connections to be projected into a common space more effectively than approaches that use linear dimensionality reduction, such as principal component analysis (see Supporting Information (SI)). The resultant components, which we describe here as 'gradients', are unitless, and identify the position of nodes along the respective embedding axis that encodes the dominant differences in nodes' connectivity patterns.

The principal gradient in humans and macaque monkeys. The principal gradient (Figure 1A), which accounts for the greatest variance in connectivity in the human brain (see Figure S1), is anchored at one end by the primary and unimodal visual, somatosensory/motor, and auditory regions. At the other end are regions including the angular gyrus, rostral anterior cingulate, posteromedial cortex, middle temporal gyrus, and middle and superior frontal gyri — regions that in humans are collectively described as the default-mode network (DMN). Regions situated between the two extreme ends of the principal gradient include the inferior frontal sulcus, intraparietal sulcus, and the inferior temporal sulcus, constituting heteromodal integration and higher-order cognitive regions.

The initial proposal of Mesulam was motivated by tract-tracing studies conducted in the macaque monkey. To determine whether our method would generalize to this form of data, we performed the same embedding analysis on a publicly available database of tract-tracing studies conducted in the macaque monkey. The principal gradient of the macaque monkey cerebral cortex is presented in Figure 1B, and, similar to the human functional connectivity-based results, is anchored at one end by visual and somatosensory/motor regions and at the other by higher-order transmodal regions in the temporal lobe and the medial and lateral prefrontal cortex. The cross-species correspondence of the principal gradient suggests this axis of connectivity variation is phylogenetically conserved, and may represent a primary dimension of cortical expansion [43].

The topography of the principal gradient in both the human and macaque monkey is consistent with the claim that cortical connectivity is organized along a dimension spanning primary/unimodal and transmodal regions — a hypothesis that is summarized schematically along the 'Gradient 1' dimension in Figure 1C. However, for this spectrum to indicate hierarchical integration across distinct modalities, the following connectivity component should distinguish between primary modalities, as indicated by the dimension 'Gradient 2' in Figure 1C.

Consistent with Mesulam's hypothesis [23, and Figure 1C], the component accounting for the second-most variance in connectivity in the human brain differentiates regions solely within the unimodal-end of the principal gradient (Figure 1D). One end of the spectrum is characterized by regions of the occipital cortex implicated in processing of visual input, while the opposite end includes the somatosensory and motor regions surrounding the central sulcus as well as the auditory regions of the temporal perisylvian region (Figure 1E). The convergence described by the first two connectivity gradients across sensory/motor modalities, and towards a singular set of nodes within transmodal cortex, is consistent with the claim that the principal gradient is organized along a dimension that integrates unimodal regions in a hierarchical manner (Figure 1C). Moreover, the principal gradient, anchored at one end by the DMN, contains within it several local processing gra-

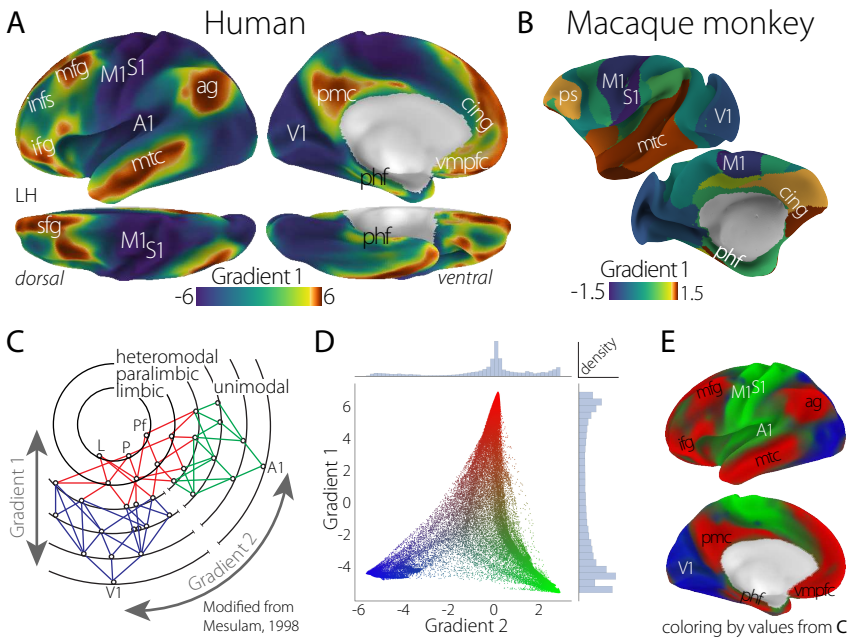

Fig. 1. The principal gradient of connectivity in both the human (A) and macaque monkey (B) cortices demonstrates a spectrum between unimodal regions (dark blue) and transmodal regions (sienna), which in the human cortex peaks in regions corresponding to the default-mode network. The proximity of colors can be interpreted as greater similarity of connectivity patterns. (C) The illustration of connectivity organization suggested by Mesulam [23] proposes a hierarchy of processing from distinct unimodal areas to integrative transmodal areas. Labels 'Gradient 1/2', which were not included in the original figure, correspond to the results in (D). (D) A scatter plot of the first two connectivity embedding gradients. Gradient 1 extends between primary sensorimotor and transmodal regions (red). Gradient 2 separates somatomotor and auditory cortex (green) from visual cortex (blue). Histograms depicting the distribution of values are presented on the respective axes. (E) Colors from the scatter plot are presented on the cortical surface for anatomical orientation. V1/A1/M1/S1, primary visual/auditory/motor/somatosensory; ag, angular gyrus; mfg/ifg/sfg, middle/inferior/superior frontal gyrus; infs, intermediate frontal sulcus, pmc, posteromedial cortex; phf, parahippocampal formation; cing, anterior cingulate cortex; vmpfc, ventromedial prefrontal cortex; mtg, middle temporal cortex, L, limbic; P, parietal; Pf, prefrontal.

dients that have already been described within the temporal and frontal lobes [12–15, 17–19]. Further gradients describing progressively less connectivity variance are available in Figure S2.

DMN peaks of the principal gradient are equidistant from primary areas. Having characterized the topography of a principal gradient in connectivity, we next investigated whether it is related to the intrinsic geometry of the cortex. To do so, we examined whether regions at the extreme of the DMN-end occupy spatial locations that are maximally distant along the cortical surface from unimodal regions. We selected 7 peak cortical nodes across the DMN clusters of the principal gradient, and calculated the minimum geodesic distance from all other nodes to any of these 'seed' nodes (see SI for further description of methods).

Figure 2 demonstrates that cortical distance reproduces many features of the spatial embedding of the principal gradient. Four of the peak DMN nodes are equidistant from the central sulcus, which is the topographical landmark of primary somatosensory/motor cortex. Likewise, we observe a similar correspondence with the calcarine sulcus, marking the location of primary visual cortex. More generally, distance clearly increases with lower principal gradient values, with an especially rapid transition in the connectivity gradient between 25–40 mm and plateaus at the extremes (Figure 2B). This relationship is nevertheless captured by a linear fit ($R^2 = 0.55$). It is noteworthy that beyond a distance of 40 mm from DMN peaks, the cortex exclusively consists of unimodal regions. In similar analyses of macaque monkey cortical distance (Figure S3), we observed a comparable distance threshold for unimodal regions. In sum, this analysis demonstrates that the principal connectivity gradient reflects macrostructural features of cortical organization: the nodes corresponding to one extreme end of the gradient — core regions of the DMN — are maximally distant from regions that directly govern perception and action.

The principal gradient captures the spatial layout of large-scale networks. We next examined the extent to which the principal gradient captures the macroscale layout of intrinsic functional connectivity networks. Despite the high reproducibility of large-scale resting-state networks [1, 44–46], there is no clear over-arching spatial schema to explain the transition of one network to another. We examined the widely-used 7-network parcellation from Yeo et al. [2] with respect to the position of each network along the principal gradient (Figure 3A). (Results using the 17-network parcellation from [2] are presented in Figure S5.)

Figure 3 demonstrates that networks are not randomly distributed along this dimension: instead, as demonstrated in the box plots of Figure 3B, cortical nodes from the same network tend to cluster at similar positions. Importantly, the DMN identified in this parcellation (red) occupies one extreme position along the principal gradient and is maximally separated from visual (purple) and motor (blue) networks, which lie at the other extreme. One exception is the limbic network (beige), which captures an extensive range of values. However, the spatial distribution of this network may be accounted for by low signal-to-noise within the original data used for parcellation [2], and it may thus not accurately reflect the connectivity of its constituent regions.

This analysis therefore demonstrates that the principal gradient of connectivity provides a framework for the spatial ordering of large-scale networks. In addition, the principal gradient captures similar, repeating transitions between these networks, which occur across cortical lobes (Figure 3C). We represent this consistent arrangement as a schematic illustration in Figure 3D. Notably, outlier gradient values for each network are located predominantly at their boundaries (Figure S4), suggesting that in some cases the principal gradient describes gradual connectivity transitions that are obscured by discrete network parcellation.

Distribution of functions along the principal gradient. Our final analysis explored whether the regions located at the DMN-

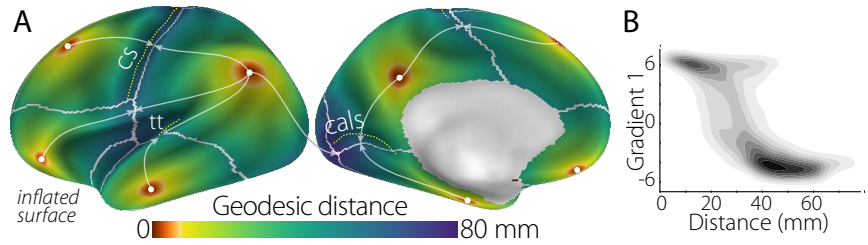

Fig. 2. (A) The minimum geodesic distance (in mm) from each point on the cortical surface to 7 seed nodes located in the positive peak of the principal gradient. Morphological landmarks of primary areas, denoted by white dotted lines, such as the central sulcus (*cs*; somatosensory/motor), calcarine sulcus (*cals*; visual), and transverse temporal gyrus (*tt*, auditory) are equidistant from the surrounding DMN peaks (illustrated by arrows). Gray lines mark the calculated equidistant line. (B) The contour scatter plot demonstrates the negative relationship between geodesic distance from the 7 positive peak locations and the principal gradient (R^2 = 0.55).

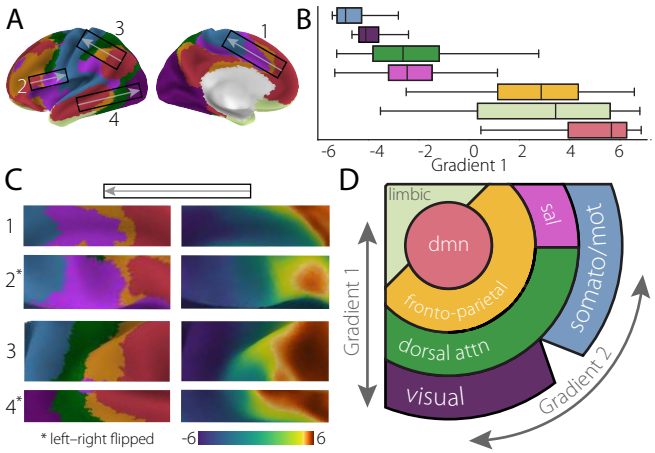

Fig. 3. (A) The principal gradient values from each of 7-networks [2] are presented as (B) box plots ordered by the mean value. (C) Illustrative cutouts taken from (A) to demonstrate the repeated patterns of network spatial adjacency captured by the principal gradient. Arrows in (A) indicate the corresponding orientation of the cutouts. (D) A schematic of the spatial relationships of canonical resting-state networks [2] applying the schema suggested by [23] presented in Figure 1C. dmn, default-mode network; sal, salience network; dorsal attn, dorsal attention network, somato/mot, somatosensory/motor network.

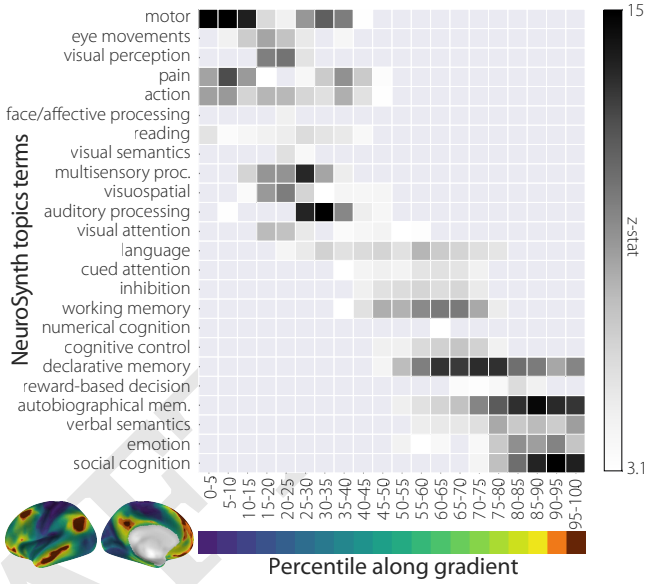

Fig. 4. NeuroSynth meta-analysis of regions-of-interest along the principal gradient using 24 topic terms. Terms are ordered by the weighted mean of their location along the gradient. Sensory processing terms are located at the top, followed by domain-general cognitive functions, and then by higher-order abstract cognitive and memory-related processes. Similar results using the BrainMap database are available in SI.

extreme of the gradient serve functions that are abstracted from perception and action. We conducted a meta-analysis using the NeuroSynth database [47] (see Figure S6 & S7 for corresponding analysis using the BrainMap database [48]), and examined the association between a list of topic terms with regions-of-interest created from 5-percentile bins of the principal gradient. Topic terms were sorted by their weighted average position along the gradient, revealing a systematic shift in function. Figure 4 demonstrates that the unimodal-end is characterized by terms depicting acting and perceiving, such as 'motor', 'visual perception', 'multisensory processing', and 'auditory processing', while the end characterized by the DMN emphasizes terms such as 'social cognition', 'verbal semantics', and 'autobiographical memory' — tasks which rely on complex representations abstracted away from specific sensory and motor processes. Between the extremes we observe domain-general functions such as 'cued attention', 'inhibition', and 'working memory' in regions corresponding to the dorsal attention and salience networks above (Figure 3D).

Discussion

Our analysis characterized a principal gradient of cortical organization in the human connectome, which is anchored at one end by systems implicated in perceiving and acting, and at the other, by transmodal association regions, corresponding in humans to the default-mode network (DMN; Figure 1). A comparative analysis using tract-tracing data from studies in the macaque monkey found a corresponding gradient, providing initial evidence that this axis of connectivity variation may be phylogenetically conserved. The observation that the principal gradient corresponds to the intrinsic geometry of the cortex — regions in the DMN have the greatest geodesic distance along the cortical surface from primary sensory-motor areas — further indicates this axis may provide a crucial blueprint for cortical organization (Figure 2). We additionally found that large-scale networks are arranged along this axis, with the same transitions between consistently adjacent networks occurring throughout the cortex (Figure 3). Finally, a task-based meta-analysis characterizing the functional attributes of this gradient showed a spectrum of increasing abstraction that follows the transition from unimodal cortex to the extreme end of the gradient in the DMN (Figure 4).

The location of the DMN at one extreme end of the principal gradient provides an organizing principle for understanding its role in cognition. First, these findings provide anatomical support for why the DMN has been associated with processes that are unrelated to immediate stimulus input, such

as daydreaming or mind-wandering [27, 28, 30]. The DMN is at a maximal distance from systems involved in perception and action in both functional connectivity and anatomical space, indicating that the neural activity in these regions is likely to be comparably insulated from direct environmental input [49, 50]. Second, the location of the DMN as equidistant from all sensory/motor systems is aligned with its broad range of functions that require integration between multiple sensory systems, including episodic [51] and semantic memory [52–54], social cognition [55, 56], goal-directed working memory tasks [26, 32, 33, 35] and reward-guided decision making [57, 58]. The two cardinal features of the DMN related to abstraction — stimulus independence and content heterogeneity — can be accounted for by its position at the end of a topographical hierarchy that is equidistant from unimodal systems, thus acting as a hub of integration across multiple sensory modalities [37] (Figure 3D).

The principal gradient illustrates a broader topographic organization of large-scale connectivity [38] that accounts for the spatial arrangement of local processing streams throughout the cerebral cortex. Gradients in both the temporal and prefrontal cortex are apparent in Figure 1, demonstrating that these hierarchies are not isolated local phenomena; they emerge as elements of a spectrum that begins within input–output systems and ends with the DMN. Notably, our results are consistent with a recent modification of the rostral–caudal processing gradient described within lateral frontal cortex [59, 60]. Rather than the more rostral areas being further along in the processing hierarchy [18, 19], two distinct hierarchical gradients of temporal- and feature-related abstraction converge in middle lateral prefrontal cortex [60]. The consistency between the principal gradient and this revised lateral prefrontal hierarchy suggests it may provide a source for future studies investigating the detailed topography of local processing streams.

In addition to incorporating local processing streams within a global framework, the principal gradient situates discrete large-scale connectivity networks along a continuous spectrum. With recent landmark advances in multimodal cortical parcellation [61], the current approach provides a complementary means to describe the gestalt of the cortical mosaic. Future studies are needed to better characterize the types of transitions between different patterns of large-scale connectivity, and to identify where processing occurs in a step-wise [11] or 'gradiential' manner [22].

It is now widely accepted that the DMN is important because it permits cognitive processing that is independent of the here and now. This capacity is adaptive because it permits flexibility: more abstract representations of a stimulus enable the generation of alternative behaviors, allowing original and creative thoughts to emerge [62]. Along those lines, a 'positive-negative' axis of brain-behavior covariation describes a similar connectivity spectrum, distinguishing the DMN from sensory/motor regions [63]. As Mesulam stated, however, the capacity for abstraction is a double-edged sword.Beyond supporting states of creativity and planning [64, 65], the DMN has also been implicated in almost all psychiatric conditions [66], indicating that there are costs, as well as benefits that accrue from the capacity to apprehend the world as it might be rather than seeing it as it is right now.

Materials and Methods

All MRI data used in this study were publicly available and anonymized. Participant recruitment procedures and informed consent forms, including consent to share de-identified data, were previously approved by the Washington University institutional review board as part of the Human Connectome Project [39].

All software used in this study is openly available at: neuroanatomyandconnectivity.github.io/gradient_analysis/

Further information regarding methods and Supporting Figures are available in the Supporting Information.

ACKNOWLEDGMENTS. Data were provided by the Human Connectome Project, WU-Minn Consortium (Principal Investigators: David Van Essen and Kamil Ugurbil; 1U54MH091657) funded by the 16 NIH Institutes and Centers that support the NIH Blueprint for Neuroscience Research; and by the McDonnell Center for Systems Neuroscience at Washington University. SG was partially supported by NIH grants 1R01EB020740-01A1, 1P41EB019936-01A1, 3R01MH092380-04S2, and 1U01MH108168-01. MP was supported by CIHR Foundation grant FDN-143212. EJ was supported by a grant from the European Research Council (283530-SEMBIND). JS was supported by European Research Council (WANDERINGMINDS–646927) and a grant from the John Templeton Foundation, "Prospective Psychology Stage 2: A Research Competition" to Martin Seligman. The opinions expressed in this publication are those of the authors and do not necessarily reflect the views of the John Templeton Foundation.

1. Damoiseaux JS et al. (2006) Consistent resting-state networks across healthy subjects. *Proc. Natl. Acad. Sci. U. S. A.* 103(37):13848–13853.
2. Yeo BTT et al. (2011) The organization of the human cerebral cortex estimated by intrinsic functional connectivity. *J. Neurophysiol.* 106(3):1125–1165.
3. Power JD et al. (2011) Functional network organization of the human brain. *Neuron* 72(4):665–678.
4. Smith SM et al. (2009) Correspondence of the brain's functional architecture during activation and rest. *Proc. Natl. Acad. Sci. U. S. A.* 106(31):13040–13045.
5. Petrides M (2005) Lateral prefrontal cortex: architectonic and functional organization. *Philos Trans R Soc Lond B Biol Sci* 360(1456):781–795.
6. Duncan J (2010) The multiple-demand (md) system of the primate brain: mental programs for intelligent behaviour. *Trends Cogn Sci* 14(4):172–179.
7. Cole MW, Yarkoni T, Repovs G, Anticevic A, Braver TS (2012) Global connectivity of prefrontal cortex predicts cognitive control and intelligence. *J Neurosci* 32(26):8988–8999.
8. Petrides M (2015) *Brain Mapping: An Encyclopedic Reference, Volume 2: Anatomy and Physiology, Systems*, ed. Toga A. (Academic Press: Elsevier), pp. 417–422.
9. Greicius MD, Krasnow B, Reiss AL, Menon V (2003) Functional connectivity in the resting brain: a network analysis of the default mode hypothesis. *Proc. Natl. Acad. Sci. U. S. A.* 100(1):253–258.
10. Raichle ME (2015) The brain's default mode network. *Annu Rev Neurosci* 38:433–447.
11. Sepulcre J, Sabuncu MR, Yeo TB, Liu H, Johnson KA (2012) Stepwise connectivity of the modal cortex reveals the multimodal organization of the human brain. *J Neurosci* 32(31):10649–61.
12. Mishkin M, Ungerleider LG (1982) Contribution of striate inputs to the visuospatial functions of parieto-preoccipital cortex in monkeys. *Behav Brain Res* 6(1):57–77.
13. Goodale MA, Milner AD (1992) Separate visual pathways for perception and action. *Trends Neurosci.* 15(1):20–25.
14. Patterson K, Nestor PJ, Rogers TT (2007) Where do you know what you know? the representation of semantic knowledge in the human brain. *Nat Rev Neurosci* 8(12):976–987.
15. Visser M, Jefferies E, Embleton KV, Lambon Ralph MA (2012) Both the middle temporal gyrus and the ventral anterior temporal area are crucial for multimodal semantic processing: distortion-corrected fMRI evidence for a double gradient of information convergence in the temporal lobes. *J Cogn Neurosci* 24(8):1766–1778.
16. Koechlin E, Ody C, Kouneiher F (2003) The architecture of cognitive control in the human prefrontal cortex. *Science* 302(5648):1181–1185.
17. Petrides M (2005) *From Monkey Brain to Human Brain. A Fyssen Foundation Symposium*, eds. S. Dehaene, J.-R. Duhamel MH, Rizzolatti G. (Cambridge, Massachusetts: The MIT Press), pp. 293–314.
18. Badre D (2008) Cognitive control, hierarchy, and the rostro-caudal organization of the frontal lobes. *Trends Cogn Sci* 12(5):193–200.
19. Badre D, D'Esposito M (2009) Is the rostro-caudal axis of the frontal lobe hierarchical? *Nat Rev Neurosci* 10(9):659–669.
20. Kaas JH (1997) Topographic maps are fundamental to sensory processing. *Brain Res Bull* 44(2):107–112.
21. Kaas JH (1987) The organization of neocortex in mammals: implications for theories of brain function. *Annu Rev Psychol* 38:129–151.
22. Goldberg E (1989) Gradiental approach to neocortical functional organization. *Journal of Clinical and Experimental Neuropsychology* 11(4):489–517. PMID: 2474566.
23. Mesulam MM (1998) From sensation to cognition. *Brain* 121 (Pt 6):1013–1052.
24. Buckner RL, Krienen FM (2013) The evolution of distributed association networks in the human brain. *Trends Cogn. Sci.* 17(12):648–665.
25. Shulman GL et al. (1997) Common blood flow changes across visual tasks: II. decreases in cerebral cortex. *Journal of Cognitive Neuroscience* 9(5):648–663.

26. Spreng RN, Grady CL (2010) Patterns of brain activity supporting autobiographical memory, prospection, and theory of mind, and their relationship to the default mode network. *J Cogn Neurosci* 22(6):1112–1123.
27. Mason MF et al. (2007) Wandering minds: the default network and stimulus-independent thought. *Science* 315(5810):393–395.
28. Christoff K, Gordon AM, Smallwood J, Smith R, Schooler JW (2009) Experience sampling during fMRI reveals default network and executive system contributions to mind wandering. *Proc Natl Acad Sci U S A* 106(21):8719–8724.
29. Stawarczyk D, Majerus S, Maquet P, D'Argembeau A (2011) Neural correlates of ongoing conscious experience: both task-unrelatedness and stimulus-independence are related to default network activity. *PLoS One* 6(2):e16997.
30. Smallwood J et al. (2016) Representing representation: Integration between the temporal lobe and the posterior cingulate influences the content and form of spontaneous thought. *PLoS One* 11(4):e0152272.
31. Weissman DH, Roberts KC, Visscher KM, Woldorff MG (2006) The neural bases of momentary lapses in attention. *Nat Neurosci* 9(7):971–978.
32. Vatansever D, Menon DK, Manktelow AE, Sahakian BJ, Stamatakis EA (2015) Default mode dynamics for global functional integration. *J Neurosci* 35(46):15254–15262.
33. Konishi M, McLaren DG, Engen H, Smallwood J (2015) Shaped by the past: The default mode network supports cognition that is independent of immediate perceptual input. *PLoS One* 10(6):e0132209.
34. Spreng RN et al. (2014) Goal-congruent default network activity facilitates cognitive control. *J Neurosci* 34(42):14108–14114.
35. Crittenden BM, Mitchell DJ, Duncan J (2015) Recruitment of the default mode network during a demanding act of executive control. *eLife* 4:e06481.
36. Krieger-Redwood K et al. (2016) Down but not out in posterior cingulate cortex: Deactivation yet functional coupling with prefrontal cortex during demanding semantic cognition. *Neuroimage*.
37. van den Heuvel MP, Sporns O (2013) Network hubs in the human brain. *Trends Cogn. Sci.* 17(12):683–696.
38. Jbabdi S, Sotiropoulos SN, Behrens TE (2013) The topographic connectome. *Curr Opin Neurobiol* 23(2):207–15.
39. Van Essen DC et al. (2013) The WU-Minn human connectome project: an overview. *Neuroimage* 80:62–79.
40. Glasser MF et al. (2013) The minimal preprocessing pipelines for the human connectome project. *Neuroimage* 80:105–124.
41. Haak KV, Marquand AF, Beckmann CF (2016) Connectopic mapping with resting-state fMRI. *arXiv preprint arXiv:1602.07100*.
42. Coifman RR et al. (2005) Geometric diffusions as a tool for harmonic analysis and structure definition of data: diffusion maps. *Proc. Natl. Acad. Sci. U. S. A.* 102(21):7426–7431.
43. Hill J et al. (2010) Similar patterns of cortical expansion during human development and evolution. *Proc Natl Acad Sci U S A* 107(29):13135–40.
44. Biswal BB et al. (2010) Toward discovery science of human brain function. *Proc. Natl. Acad. Sci. U. S. A.* 107(10):4734–4739.
45. Wang D et al. (2015) Parcellating cortical functional networks in individuals. *Nat Neurosci* 18(12):1853–60.
46. Gordon EM, Laumann TO, Adeyemo B, Petersen SE (2015) Individual variability of the system-level organization of the human brain. *Cereb Cortex*.
47. Yarkoni T, Poldrack RA, Nichols TE, Van Essen DC, Wager TD (2011) Large-scale automated synthesis of human functional neuroimaging data. *Nat. Methods* 8(8):665–670.
48. Fox PT, Lancaster JL (2002) Opinion: Mapping context and content: the brainmap model. *Nat Rev Neurosci* 3(4):319–21.
49. Kiebel SJ, Daunizeau J, Friston KJ (2008) A hierarchy of time-scales and the brain. *PLoS Comput Biol* 4(11):e1000209.
50. Friston K (2013) Life as we know it. *J R Soc Interface* 10(86):20130475.
51. Schacter DL, Addis DR (2007) The cognitive neuroscience of constructive memory: remembering the past and imagining the future. *Philos Trans R Soc Lond B Biol Sci* 362(1481):773–786.
52. Binder JR, Desai RH, Graves WW, Conant LL (2009) Where is the semantic system? a critical review and meta-analysis of 120 functional neuroimaging studies. *Cereb Cortex* 19(12):2767–2796.
53. Jefferies E (2013) The neural basis of semantic cognition: converging evidence from neuropsychology, neuroimaging and TMS. *Cortex* 49(3):611–625.
54. Constantinescu AO, O'Reilly JX, Behrens TEJ (2016) Organizing conceptual knowledge in humans with a gridlike code. *Science* 352(6292):1464–8.
55. Amodio DM, Frith CD (2006) Meeting of minds: the medial frontal cortex and social cognition. *Nat Rev Neurosci* 7(4):268–277.
56. Amft M et al. (2015) Definition and characterization of an extended social-affective default network. *Brain Struct Funct* 220(2):1031–49.
57. Fellows LK (2011) Orbitofrontal contributions to value-based decision making: evidence from humans with frontal lobe damage. *Ann N Y Acad Sci* 1239:51–8.
58. Chau BKH, Kolling N, Hunt LT, Walton ME, Rushworth MFS (2014) A neural mechanism underlying failure of optimal choice with multiple alternatives. *Nat Neurosci* 17(3):463–70.
59. Goulas A, Uylings HBM, Stiers P (2014) Mapping the hierarchical layout of the structural network of the macaque prefrontal cortex. *Cereb Cortex* 24(5):1178–94.
60. Nee DE, D'Esposito M (2016) The hierarchical organization of the lateral prefrontal cortex. *eLife* 5.
61. Glasser MF et al. (2016) A multi-modal parcellation of human cerebral cortex. *Nature*.
62. Haggard P (2008) Human volition: towards a neuroscience of will. *Nat Rev Neurosci* 9(12):934–946.
63. Smith SM et al. (2015) A positive-negative mode of population covariation links brain connectivity, demographics and behavior. *Nat Neurosci* 18(11):1565–1567.
64. Spreng RN, Stevens WD, Chamberlain JP, Gilmore AW, Schacter DL (2010) Default network activity, coupled with the frontoparietal control network, supports goal-directed cognition. *Neuroimage* 53(1):303–317.
65. Beaty RE et al. (2014) Creativity and the default network: A functional connectivity analysis of the creative brain at rest. *Neuropsychologia* 64C:92–98.
66. Broyd SJ et al. (2009) Default-mode brain dysfunction in mental disorders: a systematic review. *Neurosci Biobehav Rev* 33(3):279–96.
67. Marcus DS et al. (2011) Informatics and data mining tools and strategies for the human connectome project. *Front. Neuroinform.* 5:4.
68. Fischl B (2012) FreeSurfer. *Neuroimage* 62(2):774–781.
69. Jenkinson M, Bannister P, Brady M, Smith S (2002) Improved optimization for the robust and accurate linear registration and motion correction of brain images. *Neuroimage* 17(2):825–841.
70. Jenkinson M, Beckmann CF, Behrens TEJ, Woolrich MW, Smith SM (2012) FSL. *Neuroimage* 62(2):782–790.
71. Van Essen DC, Glasser MF, Dierker DL, Harwell J, Coalson T (2012) Parcellations and hemispheric asymmetries of human cerebral cortex analyzed on surface-based atlases. *Cereb. Cortex* 22(10):2241–2262.
72. Stephan KE et al. (2001) Advanced database methodology for the Collation of Connectivity data on the Macaque brain (CoCoMac). *Philos Trans R Soc Lond B Biol Sci* 356(1412):1159–1186.
73. Bakker R, Wachtler T, Diesmann M (2012) CoCoMac 2.0 and the future of tract-tracing databases. *Front Neuroinform* 6:30.
74. Van Essen DC (2004) Surface-based approaches to spatial localization and registration in primate cerebral cortex. *Neuroimage* 23 Suppl 1:S97–107.
75. Von Bonin G, Bailey P (1947) *The neocortex of Macaca mulatta.* (University of Illinois Press).
76. Bezgin G, Vakorin VA, van Opstal AJ, McIntosh AR, Bakker R (2012) Hundreds of brain maps in one atlas: registering coordinate-independent primate neuro-anatomical data to a standard brain. *Neuroimage* 62(1):67–76.
77. Von Luxburg U (2007) A tutorial on spectral clustering. *Statistics and computing* 17(4):395–416.
78. Tenenbaum JB, De Silva V, Langford JC (2000) A global geometric framework for nonlinear dimensionality reduction. *science* 290(5500):2319–2323.
79. Lafon S, Lee AB (2006) Diffusion maps and coarse-graining: A unified framework for dimensionality reduction, graph partitioning, and data set parameterization. *IEEE transactions on pattern analysis and machine intelligence* 28(9):1393–1403.
80. Ye AQ et al. (2015) The intrinsic geometry of the human brain connectome. *Brain Informatics*.
81. Atasoy S, Donnelly I, Pearson J (2016) Human brain networks function in connectome-specific harmonic waves. *Nature Communications* 7:10340.
82. Langs G, Golland P, Tie Y, Rigolo L, Golby AJ (2010) Functional geometry alignment and localization of brain areas. *Adv. Neural Inf. Process. Syst.* 1:1225–1233.
83. Langs G, Tie Y, Rigolo L, Golby AJ, others (2010) Localization of language areas in brain tumor patients by functional geometry alignment. *Biomarkers for Tumors*.
84. Langs G, Menze BH, Lashkari D, Golland P (2011) Detecting stable distributed patterns of brain activation using gini contrast. *Neuroimage* 56(2):497–507.
85. Langs G et al. (2011) Learning an atlas of a cognitive process in its functional geometry. *Inf. Process. Med. Imaging* 22:135–146.
86. Langs G et al. (2014) Decoupling function and anatomy in atlases of functional connectivity patterns: Language mapping in tumor patients. *Neuroimage* 103:462–475.
87. Langs G, Golland P, Ghosh SS (2015) Predicting activation across individuals with resting-state functional connectivity based multi-atlas label fusion in *Medical Image Computing and Computer-Assisted Intervention–MICCAI 2015*. (Springer), pp. 313–320.
88. Mitchell JSB, Mount DM, Papadimitriou CH (1987) The discrete geodesic problem. *SIAM J. Comput.* 16(4):647–668.
89. O'Rourke J (1999) Computational geometry column 35. *ACM SIGACT News* 30(2):31–32.
90. Fox PT, Lancaster JL, Laird AR, Eickhoff SB (2014) Meta-analysis in human neuroimaging: computational modeling of large-scale databases. *Annu Rev Neurosci* 37:409–34.
91. Laird AR et al. (2011) Behavioral interpretations of intrinsic connectivity networks. *J Cogn Neurosci* 23(12):4022–37.
92. Rottschy C et al. (2013) Differentiated parietal connectivity of frontal regions for "what" and "where" memory. *Brain Struct Funct* 218(6):1551–67.